

Pyrolysis of pine needles: effects of process parameters on products yield and analysis of products

Anil Kumar Varma¹ · Prasenjit Mondal¹

Received: 20 January 2017 / Accepted: 21 September 2017 / Published online: 17 October 2017
© Akadémiai Kiadó, Budapest, Hungary 2017

Abstract Pyrolysis of pine needles was carried out in a semi-batch reactor. The effects of pyrolysis parameters such as temperature (350–650 °C), heating rate (10 and 50 °C min⁻¹), nitrogen flow rate (50–200 cm³ min⁻¹) and biomass particle size (0.25–1.7 mm) were examined on products yield. Maximum bio-oil yield of 43.76% was obtained at pyrolysis temperature of 550 °C with a heating rate of 50 °C min⁻¹, nitrogen flow rate of 100 cm³ min⁻¹ for biomass particle size of $0.6 < d_p < 1$ mm. The characterization of pyrolysis products (bio-oil, bio-char) has been made through different instrumental methods like Fourier transform infrared spectroscopy, gas chromatography–mass spectrometry, nuclear magnetic resonance spectroscopy (¹H NMR), X-ray powder diffraction, field emission scanning electron microscope and Brunauer–Emmett–Teller surface area analysis. The empirical formula of the bio-oil and bio-char was found as CH_{1.47}O_{0.36}N_{0.005} and CH_{0.56}O_{0.28}N_{0.013} with heating value of 26.25 and 25.50 MJ kg⁻¹, respectively. Results show that bio-oil can be potentially valuable as a renewable fuel after upgrading and can be used as a feedstock for valuable chemicals production. The properties of bio-char reveal that it can be used as solid fuels, as a cheap adsorbent and as a feedstock for activated carbon production.

Keywords Biomass · Pine needles · Pyrolysis Bio-oil · Bio-char

Introduction

The world energy demand is rising rapidly due to the population growth and changing lifestyle. Currently, energy demand is mainly fulfilled by the fossil fuels such as crude oil, coal and natural gas, which contribute greenhouse gases (GHGs) emission during their combustion. To reduce the effect of global warming, acid rain due to the fossil fuels consumption, extensive efforts are going on around the world to explore the alternate sources for energy production [1]. Many countries have started their plan to replace the present energy sources with sustainable, effective, alternative and carbon neutral energy resources. Renewable energy sources such as solar, wind, hydro, geothermal and biomass are getting more attention in recent years. Among these renewable energy sources, biomass is the most sustainable and world's largest energy source with an estimated ~ 220 billion tons of dry biomass annually available in the world [2]. In future, biomass may share a major part in sustainable energy scenario and act as most promising alternative to fossil fuels. The main advantages of biomass are that it is clean, abundant, carbon neutral and economically feasible with several environmental and social benefits [3]. In addition to this, it contains very low amount of nitrogen, sulfur and ash; so it releases very less quantity of NO_x, SO_x and soot as compared to fossil fuel [4]. In India, biomass contributes about 16–18% of total energy consumption [5].

In some cases, utilization of biomass for energy production can give dual benefit by reducing environmental impacts as well as meeting the energy demand. One such example is pine needles in forests. Pine trees are abundantly available in Himalayan forests. Thus, the enormous amounts of fallen pine needles are found as waste biomass in these forests. In India, Uttarakhand has more than

✉ Prasenjit Mondal
pmpndal.iitr@gmail.com

¹ Department of Chemical Engineering, Indian Institute of Technology Roorkee, Roorkee, Uttarakhand 247667, India

340,000 hectares of pine forests, which produces nearly 2.06 million tons of pine needles per year [6]. These pine needles are serious threat to forest fires due their highly inflammable nature, and these fires damage the fertile top layer of the soil, destroy the grazing grounds for cattle and create environmental pollution as well as substantial damage to the flora and fauna, which also disturbs the ecological balance of the region. Thus, it is important to utilize the pine needles as renewable energy source for high-density biofuels production through energy efficient and cost-effective thermochemical conversion processes.

Thermochemical routes are more suitable for biofuels production from biomass, when moisture content is less. In pine needles, the moisture content is less and hence thermochemical routes can be applicable. Among different thermochemical routes such as combustion, pyrolysis and gasification, pyrolysis is the most promising as it can convert biomass/organic materials into liquid product (bio-oil), solid char (bio-char) and non-condensable gases (NCGs) by heating in inert atmosphere [7, 8]. In pyrolysis process, the relative yield of different products depends upon many operating parameters like reactor types, pyrolysis temperature, heating rate and residence time [9]. Reactor types such as (batch, semi-batch and continuous) as well as biomass composition and properties like particle size, density also play significant role on the quality and quantity of different products [10]. It has been proved that high heating rate and low residence time (fast pyrolysis) generate more liquid products yield than that of low heating rate and long residence time (slow pyrolysis) [11]. Further, continuous reactor can give more bio-oil production rate per unit reactor volume than batch and semi-batch reactor. However, complexity of operation is maximum in continuous reactor, and design of continuous reactor requires more understanding of the process. Moreover, when a new biomass is used, batch and semi-batch reactors are utilized to investigate the process characteristics and generate data for kinetics and reactor design. Normally, the feedstock is initially investigated through thermogravimetric analysis (TGA) to generate kinetic data and identify suitable temperature and heating rate for pyrolysis [12]. Thereafter, batch and semi-batch reactors are used to compute the design parameters for continuous reactors. Although, fast pyrolysis produces more liquid product, it requires more complex reactor and controlled operation. Therefore, it seems that both fast and slow pyrolysis should be explored, and slow pyrolysis may be attractive if char utilization options can give value addition to the process. It is also interesting that the quality of the products like bio-oil, bio-char and gas also depends on the feedstock properties and operating conditions [9].

In the literature, pyrolysis of different types of biomass such as hornbeam shell [3], hazelnut bagasse [4], sunflower-extracted bagasse [13], bamboo biomass [14],

cotton stalk waste [15], napier grass [16], pine sawdust [10, 17] and mango seed waste [18] has been investigated in different types of reactors (batch, semi-batch and continuous). In most of these literatures, the effects of various operating parameters on products yield have been studied. However, analysis of the products quality is not carried out in all the literatures. Further, although pyrolysis of pine wood sawdust has been studied earlier [19–23], however, pyrolysis of pine needles has not been reported in the literature. Only few reports are available on the TG analysis and kinetic evaluation of pine needles [6, 24–27].

In the present study, pyrolysis of pine needles is done in a semi-batch reactor for production of bio-oil, bio-char and pyro gas. The effects of pyrolysis temperature, heating rate, particle size range and nitrogen (N_2) flow rate on the pyrolysis products yield are investigated. In addition, it provides the comprehensive information about various physical, chemical and fuel properties of bio-oil and bio-char, as well as analyzes the composition of pyro gas and discusses the different ways for utilization of these products. It also critically analyzes with some recently reported literature on pyrolysis of different biomass to assess the suitability for pyrolysis of pine needles.

Materials and methods

Raw materials

The pine needles used in this study were collected from IIT Roorkee campus, India. Prior to use, pine needles were sun dried for 2 days, grounded in Wiley grinder and different particle size range of $d_p < 0.25$, $0.355 < d_p < 0.6$, $0.6 < d_p < 1$, $1 < d_p < 1.7$ and $d_p > 1.7$ mm were prepared by using Indian standard (IS) sieve. The sample fractions were stored in airtight polyethylene bags. All the samples were dried in hot air oven before analysis and pyrolysis experiments. Figure 1 shows the photographs of raw pine needles, milled pine needles and bio-oil from pyrolysis.

Different techniques used for characterization of biomass, bio-oil and bio-char

Characteristics of biomass, bio-oil and bio-char were determined by various techniques as described below.

Proximate and ultimate analysis

Proximate analysis of pine needles and bio-char was done to find out moisture, volatile matter, ash and fixed carbon content by standard methods [6]. Ultimate analysis of pine needles, bio-oil and bio-char was carried out by elemental analyzer (Elementar Vario EL III model).

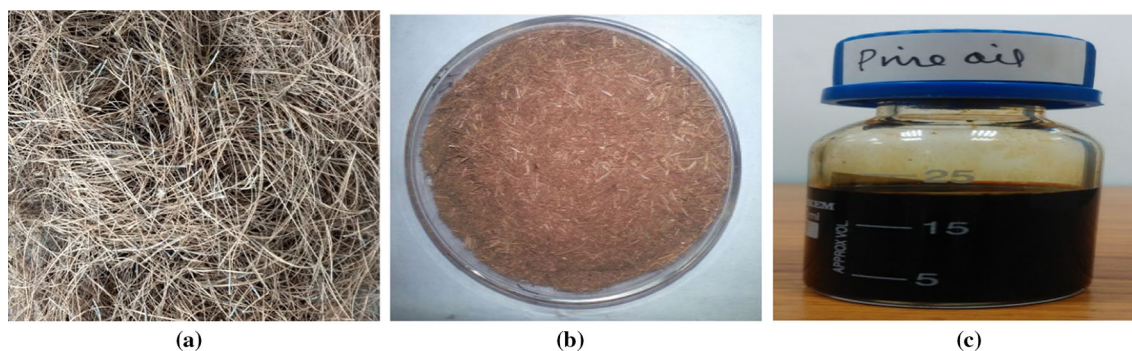


Fig. 1 Photograph of **a** raw pine needles, **b** milled pine needles and **c** bio-oil

Lignocellulosic composition

Lignocellulosic composition of biomass such as cellulose, hemicellulose, lignin and extractives was determined by analytical methods [28].

Calorific value, fuel and physical properties

Higher heating value (HHV) of pine needles, bio-oil and bio-char were determined in a Parr 6300 bomb calorimeter. Fuel and other physical properties of bio-oil such as density, kinematic viscosity, flash point, pour point and Conradson carbon residue (CCR) was determined by the standard methods. The pH of bio-oil and bio-chars was measured by using a pH meter (pH meter CL 46⁺ of Toshcon Industries, India). For measuring the pH of bio-char, sample was mixed with deionized water with ratio of 1:20 (w/v) and shaking with 180 rpm for 24 h to form homogeneous suspension and then pH was measured [29].

Thermal analysis

Thermal analysis of pine needles and bio-char was carried out by thermal analyzer (Model-SII 6300 EXSTAR), where simultaneous thermogravimetric (TG), derivative thermogravimetric (DTG) and differential thermal analysis (DTA) curves were obtained. The analysis were done in the temperature range of 30–800 °C with heating rate of 10 °C min⁻¹ under N₂ atmosphere with flow rate of 200 mL min⁻¹ for pine needles and in air atmosphere for bio-char with flow rate of 200 mL min⁻¹.

FTIR analysis

The organic functional groups present in bio-oil and bio-char were analyzed by Thermo Scientific Nicollet 6700 FTIR spectrometer using pellet technique. Where small amount of dried bio-char sample was mixed with KBr and pressed under vacuum to form pellets and for bio-oil small

drop of sample was put on KBr pellet and then analyzed. Fourier transform infrared (FTIR) spectrum of bio-oil and bio-char was developed under transmittance mode with wavenumber range of 4000–500 cm⁻¹.

GC-MS analysis

Gas chromatography–mass spectrometry (GC–MS) analysis of bio-oil was done with an Agilent 6850 GC equipped with an Agilent 7890 MS, using a HP-5 capillary column (30 m × 0.25 mm) with 0.25-μm film thickness to identify the volatile compounds present in the bio-oil. GC–MS was programmed as GC oven temperature hold at 50 °C for 4 min, then heated up to 280 °C with heating rate of 4 °C min⁻¹ and hold there for 20 min. Injector and detector temperatures were 250 and 280 °C, respectively. The MS was fixed at ionization energy of 70 eV with mass electron (m/z) range of 50–550. Split ratio of 1:10 was used in the injection of 1 μL sample solution, and helium was used as a carrier gas with flow rate of 1 mL min⁻¹. The compounds were identified using National Institute of Standards and Technology (NIST) library of mass spectra data base.

¹H NMR analysis

A proton nuclear magnetic resonance (¹H NMR) spectrum of bio-oil was obtained by NMR spectrometer (Model Avance 500 Bruker-Biospin, Switzerland) using deuterated chloroform (CDCl₃) as solvent to determine the types of proton present in bio-oil. Quantification of different types of protons was done on the basis of percentage area of the peaks found for different region corresponding to different types of compounds like aliphatic, olefinic, aromatics, alcohols and phenols.

Analysis of gaseous products

Gaseous products were collected in Tedlar bags during the experiments and analyzed by gas chromatograph (NEW-CHROME 6800 gas chromatograph) coupled with a thermal conductivity detector (TCD). A stainless steel column (2.0 m × 3.175 mm) packed with Porapack-Q (80–100 mesh) was used. The carrier gas was argon at a flow rate of 30 mL min⁻¹ at 75 psi pressure. The injected volume of sample was 60 μL, and operational conditions were as follows: injector temperature: 80 °C, oven temperature: 50 °C and detector temperature: 90 °C. The standard gas mixture of H₂, CO, CO₂ and CH₄ was used as the internal standard for quantification.

XRD analysis

The XRD analysis of pine needles and bio-char was conducted in a BRUKER X-ray diffractometer (model D8 advance) operating at 40 kV and 30 mA, with scanning rate of 1° per min using Cu-K α radiation source at 1.54 Å with angle 2 θ of 5°–90°.

FESEM analysis

Field emission scanning electron microscope (Carl Zeiss Ultra Plus) equipped with energy-dispersive X-ray spectrometer (EDX) was used to study the surface morphology and to investigate the surface elemental composition of bio-char.

Surface area and pore volume analysis

The microscopic surface area and pore volume distribution of bio-char were measured by nitrogen adsorption/desorption method using Micromeritics ASAP 2020 instrument by Brunauer–Emmett–Teller (BET) and Barrett–Joyner–Halenda (BJH) methods.

Experimental setup

The pyrolysis experiments of pine needles were conducted in a laboratory scale semi-batch pyrolysis reactor. Figure 2 shows the schematic diagram of experimental setup. Reactor is a cylindrical shape vessel made of 316 stainless steel with height of 16 cm and diameter of 5 cm. The reactor was externally heated by electrical furnace with 2 kW power. Temperature inside the reactor was controlled by using external PID controller. The reactor had two openings at upper section, one opening was used for continuous supply of N₂ for inert atmosphere and another opening for outlet of reactor through which hot vapors come out and a glass condenser attached at the outlet to

condense these vapors. Ice-cooled water was circulated in the condenser as a cooling medium through the pump. The condensed liquid products were collected in measuring cylinder and weighted for yield. The gaseous products were collected in the Tedlar bags for analysis. After pyrolysis, the reactor was cooled to room temperature and residue left as solid char was collected and weighed. The gaseous products yield was calculated by material balance as a difference between total biomass fed and sum of bio-oil and bio-char yield.

Experimental

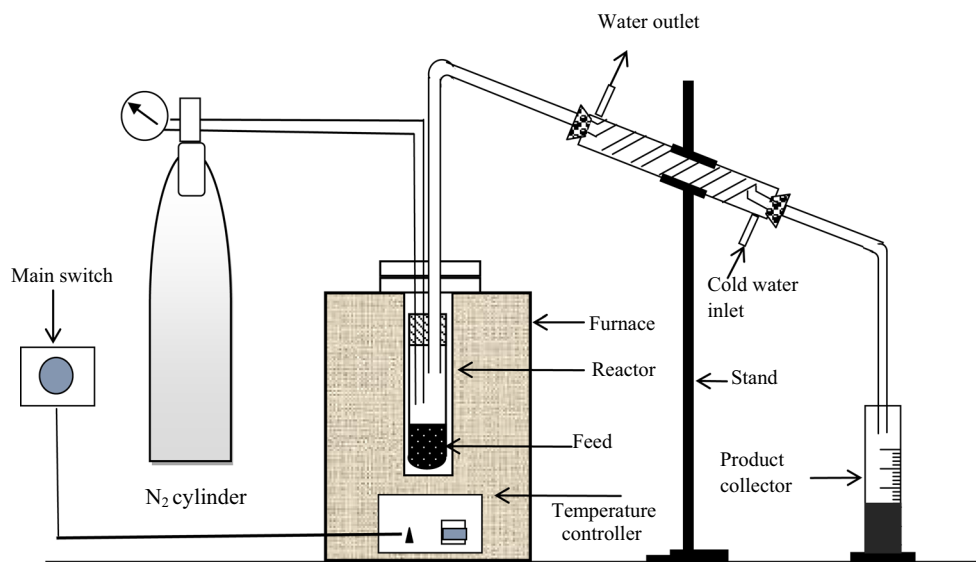
The pyrolysis experiments were categorized into three groups to investigate the effect of pyrolysis parameters on products yield and to find out the optimum parameters for maximum bio-oil yield. For each group of experiments, 15 g of pine needles sample was taken into the reactor and then closed tightly. Before each experiment, N₂ was purged with flow rate of 100 cm³ min⁻¹ for 10 min to provide inert atmosphere inside the reactor. In the first group of experiments, effect of temperature and heating rate on the products yield were investigated. Dried pine needles sample with particle size of 0.6 < d_p < 1 mm was taken in reactor, and temperature was separately raised at heating rates of 10 and 50 °C min⁻¹ to reach the final temperature of 350, 400, 450, 500, 550, 600 and 650 °C, and flow rate of N₂ was constant at 100 cm³ min⁻¹. At each of final temperature, experiment was continued for additional 30 min to ensure the total conversion of biomass or no further release of significant amount of vapors observed at outlet.

In the second group, experiments were done to find out the effect of particle size on the products yield. The experiments were carried out with five different particle size ranges of $d_p < 0.25$, $0.355 < d_p < 0.6$, $0.6 < d_p < 1$, $1 < d_p < 1.7$ and $d_p > 1.7$ mm, at final temperature of 550 °C, heating rate of 50 °C min⁻¹ and N₂ flow rate of 100 cm³ min⁻¹.

The third group of experiments was carried out to investigate the effect of N₂ flow rate on the products yield. The experiments were performed with four different N₂ flow rate of 50, 100, 150 and 200 cm³ min⁻¹ at constant pyrolysis temperature of 550 °C, heating rate of 50 °C min⁻¹ and particle size of 0.6 < d_p < 1 mm.

All pyrolysis experiments were performed thrice, and average values have been reported, with the error limit of ± 0.5 in absolute value.

Fig. 2 Systematic diagram of experimental setup



Results and discussion

Characteristics of biomass

Table 1 summarizes the proximate and ultimate analysis, empirical formula and calorific value of pine needles and bio-char. Proximate analysis is used to explore the fuel quality of solid biomass. High volatile matter with low ash and moisture content biomass are more favorable for the production of bio-oil through pyrolysis [30]. High volatile content (77.55%) of pine needles reveals the possibility of higher bio-oil yield. It has low ash content of 3.38%. In

addition, pine needles have low moisture content of 5.3%. It is mentioned that for pyrolysis process the moisture content should be less than 10% as well as high moisture requires additional heat and reduces the thermal efficiency of biomass [30]. Fixed carbon calculated by difference is 13.77%. Ultimate analysis of pine needles shows the C, H, O, N and S contents are 46.38, 7.08, 46.02, 0.45 and 0.07%, respectively. This result shows that S and N contents are very low, so the emission of toxic gases like SO_x and NO_x is likely to be very low. The H/C and O/C molar ratios of present pine needles are found as 1.83 and 0.74, respectively. The empirical formula of pine needles is found as CH_{1.83}O_{0.74}N_{0.008} by ultimate analysis data. The lignocellulosic analysis of pine needles shows the cellulose, hemicelluloses, lignin and extractives contents are 34.5, 29.1, 31.7 and 4.7%, respectively. The HHV of pine needles is 19.65 MJ kg⁻¹, which is comparable with other biomass used in pyrolysis [30]. The above analysis of pine needles shows that it has potential for use as feedstock for pyrolysis.

Table 1 Main characteristics of the pine needles and bio-char

Characteristics	Pine needles	Bio-char
Proximate analysis/%		
Moisture	5.30	1.14
Volatile matter	77.55	18.36
Ash	3.38	15.16
Fixed carbon*	13.77	65.34
Ultimate analysis/%		
Carbon (C)	46.38	69.83
Hydrogen (H)	7.08	3.28
Nitrogen (N)	0.45	1.07
Sulfur (S)	0.07	0.03
Oxygen* (O)	46.02	25.79
O/C molar ratio	0.74	0.28
H/C molar ratio	1.83	0.56
Empirical formula	CH _{1.83} O _{0.74} N _{0.008}	CH _{0.56} O _{0.28} N _{0.013}
Higher heating value/ MJ kg ⁻¹	19.65	25.50

* By difference

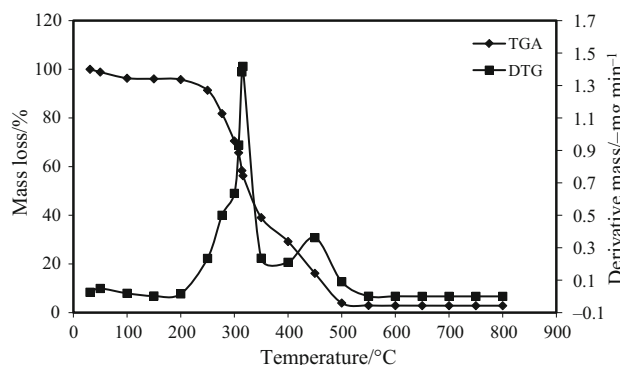


Fig. 3 TG/DTG curves of pine needles at a heating rate of 10 °C min⁻¹

Thermal behavior of pine needles is shown in Fig. 3. Thermal degradation of present pine needles occurs into four stages as observed from thermogravimetric (TG) and derivative thermogravimetric (DTG) curves. The first stage of thermal degradation starts from temperature of 32 °C to about 200 °C, in which $\sim 5\%$ of mass loss occurs due to the removal of moisture present in biomass sample [8]. The second stage observes within the temperature range of 200–340 °C with maximum mass loss of $\sim 53\%$. For this stage, DTG curve also shows a peak with maximum rate of mass loss $\sim 1.42 \text{ mg min}^{-1}$ at 317 °C. Mass loss during this stage is due to the degradation of hemicellulose and cellulose. Due to the high rate of mass loss, this section is termed as active pyrolysis stage [8, 31]. Further, third stage occurs in the temperature range of 340–500 °C with mass loss of around 38% and for this stage DTG curve denotes the rate of mass loss 0.36 mg min^{-1} at 451 °C. Mass loss during this section is the result of thermal decomposition of cellulose and some lignin, and this section also signifies as active pyrolysis stage. Moreover, for last stage above 500 °C rate of degradation decreases and becomes almost constant up to 800 °C, mass loss during this stage is very low ($\sim 2\%$). Degradation of lignin occurs during this stage. Very low amount ($\sim 2\%$) of residue is left after 800 °C. This stage is referred as passive pyrolysis. It is evident from previous literature that the decomposition of hemicellulose, cellulose and lignin occurs in the temperature range of 210–315, 315–400 and 150–900 °C, respectively [32]. Pyrolysis temperature is preferred for the experiments in semi-batch reactor based on above data. Based on the available literature, the pyrolysis temperature for most of the biomass lies in the range of 350–700 °C, and for pyrolysis of other biomass it varies as 400–600 °C for hornbeam shell [3], 350–600 °C for perennial grass [8] and 400–700 °C for sunflower-extracted bagasse [13].

Effect of operating parameters on the products yield

The effect of operating parameters such as temperature, heating rate, nitrogen flow rate and particle size of biomass on the pyrolysis products yield (bio-oil, bio-char and pyro gas) is discussed below.

Effect of pyrolysis temperature and heating rate on the products yield

Figure 4a, b shows the products yield for pyrolysis of pine needles with heating rates of 10 and 50 °C min⁻¹ in relation to final pyrolysis temperatures of 350, 400, 450, 500, 550, 600 and 650 °C, for biomass particle size of $0.6 < d_p < 1 \text{ mm}$ and N₂ flow rate of 100 cm³ min⁻¹. The yield of pyrolysis products greatly depends upon the pyrolysis temperature. The main role of temperature is to

provide the required heat for decomposition and fragmentation of biomass. For pyrolysis, higher bio-oil yield is found at intermediate temperature between 350 and 600 °C. During pyrolysis, initially the yield of bio-oil increases with increase in temperature reaches a maximum value and decreases thereafter. Similar type of results is also found in the present study. At lower heating rate of 10 °C min⁻¹, the yield of bio-oil increases from 25.81 to 42.35% as the pyrolysis temperature rises from 350 to 550 °C and decreases thereafter to 39.12% as the temperature increases to 650 °C. At heating rate of 50 °C min⁻¹, it increases from 27.12 to 43.76% as pyrolysis temperature rises from 350 to 550 °C and with further increase in temperature up to 650 °C, the yield of bio-oil decreases to 39.42%. Maximum yield of bio-oil found at temperature of 550 °C for both the heating rates (10 and 50 °C min⁻¹). In addition to this, the yield of bio-char decreases from 56.05 to 27.74% for heating rate of 10 °C min⁻¹ and 52.42–23.14% for heating rate of 50 °C min⁻¹ as temperature increases from 350 to 650 °C. Bio-char yield always decreases with increase in temperature, and heating rate due to the significant loss of volatile matter or secondary decomposition of char occurs at higher temperature [33]. As it is observed from Fig. 4a, b, the yield of gaseous products increases with increase in temperature and it is maximum at higher temperature of 650 °C. This is due to the fact that at higher temperature secondary cracking reactions of pyrolysis vapors as well as secondary decompositions of char occur, which increases non-condensable gaseous products yield and subsequently reduces the bio-oil yield [34]. From the above discussion; it is proven that yield pattern of pyrolysis products is significantly influenced by the pyrolysis temperature. For the present study, maximum bio-oil yield of 43.76% is found at pyrolysis temperature of 550 °C and heating rate of 50 °C min⁻¹.

Effect of particle size on the products yield

Figure 5 shows the effect of biomass particle size on products yield at constant pyrolysis temperature of 550 °C, heating rate of 50 °C and N₂ flow rate of 100 cm³ min⁻¹. For smaller particle size of $d_p < 0.25 \text{ mm}$, bio-oil yield is found as 39.17% and for larger particle size of $d_p > 1.7 \text{ mm}$, bio-oil yield is found as 38.48%. The difference in bio-oil yield for smaller and larger size particle is very less. So, for present study no significant effect of particle size on bio-oil yield is found. However, as the particle size increases from $d_p < 0.25 \text{ mm}$ to the range of $d_p > 1.7 \text{ mm}$, the yield of bio-char increases from 27.96 to 37.25%. The variation in gas yield with particle size shows that the minimum gas yield of 24.26% found for $d_p > 1.7 \text{ mm}$ and maximum gas yield of 32.87% found for $d_p < 0.25 \text{ mm}$.

Fig. 4 Effect of pyrolysis temperature on products yield at heating rate of **a** $10\text{ }^\circ\text{C min}^{-1}$, **b** $50\text{ }^\circ\text{C min}^{-1}$, with particle size of $0.6 < d_p < 1\text{ mm}$ and N_2 flow rate of $100\text{ cm}^3\text{ min}^{-1}$

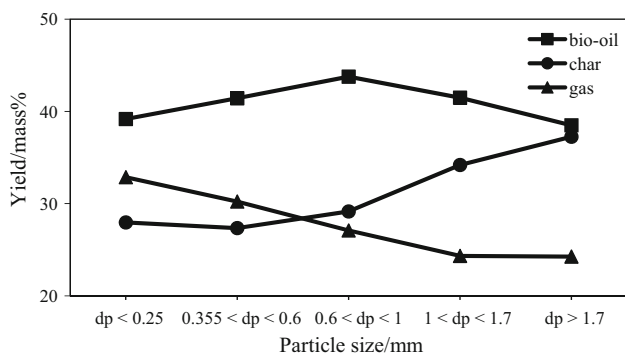
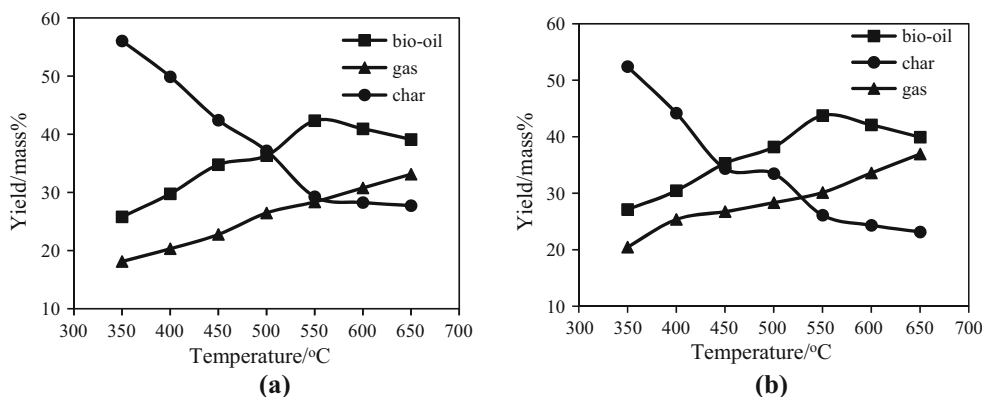


Fig. 5 Effect of particle size on the products yield at pyrolysis temperature of $550\text{ }^\circ\text{C}$, heating rate of $50\text{ }^\circ\text{C min}^{-1}$ and N_2 flow rate of $100\text{ cm}^3\text{ min}^{-1}$

This occurs because for larger size particles greater temperature gradients exist inside it, which probably increases the char yield and decrease the bio-oil and gaseous products yield [34]. According to the experimental results, maximum bio-oil yield of 43.76% is found for particle size range of $0.6 < d_p < 1\text{ mm}$ with bio-char yield of 29.15%.

It is well known that biomass is a poor conductor of heat, which poses hurdle in heat transfer during pyrolysis [9]. The suitable particle size of biomass for pyrolysis depends upon the type of pyrolysis process and nature of biomass. Generally, small particle size is preferred for rapid pyrolysis since it heats up uniformly and produces higher amount volatile matter as well as increases the bio-oil and gaseous products yield. In contrast, large particle size accounts for high-temperature gradient inside the particle resulting poor heat transfer to inner surface of the particle and possibly increases the char yield and subsequently decreases the bio-oil and gaseous products yield [35]. Further, large size particles require high activation energy, which results to the heat transfer limitation [36].

Effect of nitrogen gas flow rate on the products yield

The variation of products yield with N_2 flow rates is shown in Fig. 6. Flow rate of N_2 plays an important role in the pyrolysis process. It creates the inert atmosphere for pyrolysis and also reduces the residence time for hot pyrolysis vapor and minimizes the probability of repolymerization of vapors to maximize the bio-oil yield [37]. Moreover, this requires the rapid quenching of hot pyrolysis vapors [38].

Figure 6 reveals that the yield of bio-oil is found as 40.12% with N_2 flow rate of $50\text{ cm}^3\text{ min}^{-1}$ and it increases to 43.76% with N_2 flow rate of $100\text{ cm}^3\text{ min}^{-1}$ and decreases thereafter to 40.03% for $200\text{ cm}^3\text{ min}^{-1}$. This is due to the fact that at higher N_2 flow rate, volatile components are flown out from reactor with N_2 stream without proper condensation [3]. The char yield decreases from 35.74 to 27.19% and gas yield increases from 24.14 to 32.78% as N_2 flow rate increases from 50 to $200\text{ cm}^3\text{ min}^{-1}$. So, it concludes that char yield decreases and gaseous products yield increases with N_2 flow rate. Maximum bio-oil yield of 43.76% is found at N_2 flow rate of $100\text{ cm}^3\text{ min}^{-1}$. From the available literature, it is revealed that bio-oil yield is not much influenced by N_2 flow rate. Demiral and Sensoz [4] observed that 3.3%

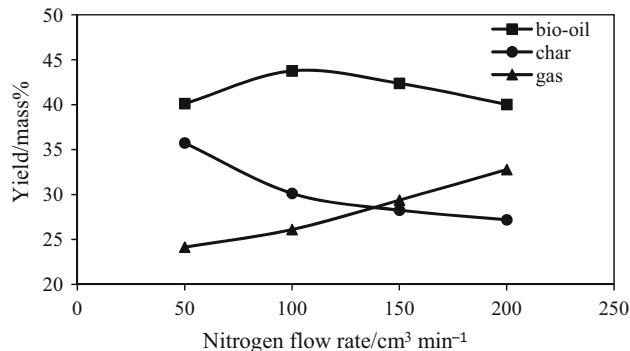


Fig. 6 Effect of N_2 flow rate on products yield at pyrolysis temperature of $550\text{ }^\circ\text{C}$, heating rate of $50\text{ }^\circ\text{C min}^{-1}$ and particle size of $0.6 < d_p < 1\text{ mm}$

more liquid oil obtained at $150 \text{ cm}^3 \text{ min}^{-1}$ than at $50 \text{ cm}^3 \text{ min}^{-1}$ of N_2 flow rate. Acikgoz et al. [39] reported only 3% extra liquid oil found by increasing N_2 flow rate from 50 to $100 \text{ cm}^3 \text{ min}^{-1}$. It is also prominent that at very high N_2 flow rate basically decreases the bio-oil yield. However, low N_2 flow rate is proficient to achieve maximum bio-oil yield [40].

Table 2 shows the comparative study of the pyrolysis of different types of biomass in semi-batch and fixed bed reactor system. It reports the optimum operating parameters (temperature, heating rate, biomass particle size and N_2 flow rate) for pyrolysis of pine needles and other biomass for maximum bio-oil yield. It is observed that the optimum pyrolysis temperature, heating rate, biomass particle size and N_2 flow rate mainly vary in the range of 500–600 °C, 10–50 °C min^{-1} , 0.5–1 mm and 100–200 $\text{cm}^3 \text{ min}^{-1}$, respectively, and bio-oil yield varies in the range of 30–66 mass% except for pyrolysis of hornbeam shell (24.67 mass%) and perennial grass (26.18 mass%). The variation in the bio-oil yield may be due to the variation in the properties of biomass as well as operating conditions.

Characteristics of bio-oil

The energy value of a fuel mainly depends upon the carbon and hydrogen content, so the elemental analysis of bio-oil

is important to be mentioned. In the present study, C and H contents in bio-oil are 62.14 and 7.63%, respectively, whereas these values for pine needles are 46.38 and 7.08%, respectively. This indicates that the bio-oil contains more C and H than the biomass. The measurement of N and S in fuel is also very essential for environmental point of view, because burning of fuel which contains N and S produces their oxides, which are responsible for environmental pollution. In the present study, bio-oil contains very less amount of N and S. The oxygen content in bio-oil (30%) is lower than the original feedstock (46.38%), and it is important that lower oxygen content is favorable for good fuel and also increases the heating value of fuel. However, it has higher oxygen content than petroleum fuels. High oxygen content in bio-oil signifies the presence of several highly polar compounds prominent to high viscosity and boiling point [45]. The H/C and O/C molar ratio of pine needles bio-oil is 1.47 and 0.36, respectively. Molar ratio of H/C in bio-oil is lower than light and heavy crude oils (1.5–1.7). This ratio should be increased in the range of 1.9–2.0 for transportation fuel. So, upgradation of bio-oil by hydrotreating can be used to increase this ratio by adding hydrogen [51]. For promising use of bio-oil to energy application, molar ratio of O/C should be low and H/C should be high. The empirical formula of present bio-

Table 2 Comparative study for pyrolysis of different types of biomass

Biomass	Reactor type	Temperature/ °C	Heating rate/ C min^{-1}	Particle size/ mm	N_2 flow rate/ $\text{cm}^3 \text{ min}^{-1}$	Bio-oil yield/mass%	References
Pine needles	Semi-batch	550	50	0.6–1	100	43.76	Present study
Hornbeam shell	Fixed bed	550	50	0.5–1	100	24.67	[3]
Perennial grass	Fixed bed	500	40	0.2	150	26.18	[8]
Napier grass stem	Fixed bed	600	30	0.2–2	30	32.26	[16]
Sugarcane bagasse	Fixed bed	500	50	0.5–1.0	200	66.1	[30]
Olive bagasse	Fixed bed	500	10	0.425–0.6	150	37.7	[34]
Jatropha curcas cake	Fixed bed tubular	550	5	0.5–0.8	100	45	[41]
Paulownia wood	Fixed bed reactor	500	50	0.425–1	100	54	[42]
Safflower seed press cake	Fixed bed	500	50	1.8 (avg)	100	36.1	[43]
Coconut shell	Semi-batch	575	20	< 1	–	49.5	[44]
Grape bagasse	Fixed bed	550	50	–	100	41.60	[45]
Napier grass	Induction heating	500	100	0.224 (avg)	–	35.7	[46]
Sal seed	Semi-batch	600	20	–	–	52.8	[47]
Oil palm residues	Fixed bed tubular	600	30	–	30	34.26	[48]
Mahua seed	Semi-batch	525	20	0.55–1	30	49	[49]
Sugarcane bagasse	Fixed bed	560	30	0.5–0.85	116	53.38	[50]

Table 3 Comparison of ultimate analysis, physical and fuel properties of present bio-oil and other pyrolytic oils and petroleum product

Pyrolysis oil	Properties											
	Ultimate analysis/%					Density at 15 °C/ kg m ⁻³	Kinematic viscosity at 40 °C/cSt	Flash point/ °C	Pour point/°C	pH	HHV/ MJ kg ⁻¹	References
	C	H	N	S	O*							
Pine needles	62.14	7.63	0.39	0.02	29.82	1062	12.54	61	- 10	3.4	26.25	Present study
Hornbeam shell	66.42	6.93	1.54	-	25.11	1056	1.4	-	-	-	30	[3]
Perennial grass	47.95	7.23	0.3	-	44.52	951	-	43	+ 4	3.8	24.7	[8]
Napier grass stem	27.50	9.57	0.84	0.14	24.7	1030	2.45	-	-	2.4	25.30	[16]
Olive bagasse	66.9	9.2	2.0	-	21.9	1070	51	77	-	-	31.8	[34]
Jatropha curcas cake	53.68	10.43	2.71	0.05	32.98	1100	-	180	- 6	-	25.91	[41]
Coconut shell	59.14	5.47	4.21	0.34	30.84	1053	1.47	-	-	-	19.75	[44]
Grape bagasse	71.72	8.69	2.69	-	16.90	992	23	61	-	-	32.95	[45]
Oil palm residues	32.96	6.99	0.01	0.19	59.85	1020	2.06	-	-	3.2	19.24	[48]
Mesua ferrea seed cover	56.12	6.97	1.83	-	31.87	958	-	42	+ 4	3.9	24.91	[54]
Pongamia glabra seed cover	60.05	7.11	1.45	-	29.08	972	-	50	+ 7	3.7	32.63	
Sugarcane bagasse	50.01	6.5	0.85	0.08	42.31	1160	18.80	103	- 16	2.9	21.85	[55]
Rice straw	42.3	6.53	-	-	50.96	1153	10.81	103	- 8	3.0	18.34	[56]
Diesel	85.72	13.2	0.18	0.3	0.6	820–850	2–5.5	53–80	- 40 to - 1	5.6	42–45	[44]

*By difference

oil obtained from ultimate analysis data is $\text{CH}_{1.47}\text{O}_{0.36}\text{N}_{0.005}$.

Physical and fuel properties such as density, kinematic viscosity, flash point, pour point, CCR, pH and calorific value of bio-oil are important for assessing and determining the feasibility of bio-oil as liquid fuel. Pine needles bio-oil is dark brown in color and has smoky smell. The density of pine needles bio-oil is found as 1062 kg m^{-3} at $15 \text{ }^\circ\text{C}$, which is approximately similar to the other pyrolytic oils obtained from olive bagasse [34], coconut shell [44], grape bagasse [45] and rice husk [52]. Viscosity of present bio-oil is high (12.54 cSt at $40 \text{ }^\circ\text{C}$) as compared to conventional fuels. High density and viscosity of bio-oil may create difficulties in pumping and atomization of fuel in the engine and also affect the combustion quality of bio-oil. Thus, further treatment such as upgradation and refining is required to meet the desired quality similar to diesel and heavy fuel oil. Flash point of bio-oil is $61 \text{ }^\circ\text{C}$, and it is in a comparable range with other bio-oils and petroleum fuels as well as it ensure its safe storage. Pour point of bio-oil ($- 10 \text{ }^\circ\text{C}$) is acceptable for most of the climatic conditions. CCR value is 4.52% . The pH of bio-oil is found as 3.40 . It is acidic in nature due to the presence of organic acids,

aldehydes and phenols. Due to the low pH, bio-oil becomes highly unstable and corrosive to mild steel and aluminum [53]. Therefore, some chemical treatment of bio-oil is required to lower the acidity, and suitable selection of materials is required for piping and storage. HHV of pine needles bio-oil is 26.25 MJ kg^{-1} , which is comparable to the other pyrolytic oils. However, it is lower than the diesel ($42\text{--}45 \text{ MJ kg}^{-1}$) because it comprises more oxygen content than petroleum crude.

Table 3 shows the comparison of ultimate analysis, physical and fuel properties of present bio-oil and other pyrolytic oils and petroleum product. From Table 3, it is evident that the present bio-oil has comparatively higher C, H and lower O content than other bio-oils as well HHV is comparable to the other bio-oils. It is also interesting to note that the present study shows more extensive characteristics including HHV, density, viscosity, flash point, pour point and CCR of bio-oil. In many literatures as reported in Table 3, fuel characterization is not complete. On the basis of the above information, it can be concluded that the present process is highly competitive to the others as reported in Table 3 and shows better bio-oil characteristics.

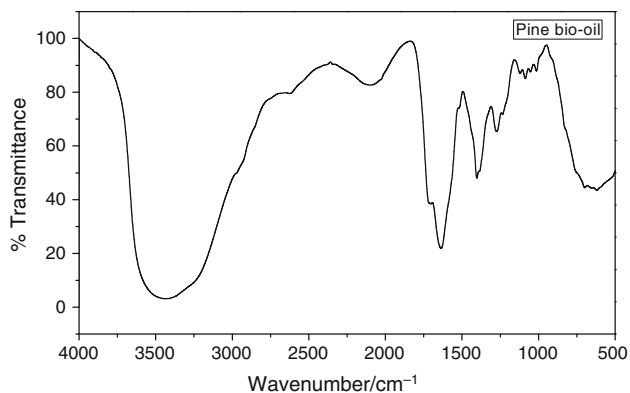


Fig. 7 FTIR spectra of bio-oil

The quality of bio-oil depends upon their chemical composition. Bio-oil obtained from pyrolysis of pine needles contains the mixture of various unknown chemical compounds. Therefore, chemical analysis of bio-oil is very important. Bio-oil is composed of thermally decomposed products of cellulose, hemicellulose and lignin. Pyrolysis of cellulose follows two parallel pathways as depolymerization and fragmentation of the ring scission. The depolymerization mainly produces levoglucosan (LG), cyclopentanones, furans, pyrans and other related derivatives. Ring scission mostly produces hydroxyacetaldehyde (HAA), acetol (HA), esters and other linear alcohols. Pyrolysis of hemicellulose as xylan mainly produces water, acids (formic acid, acetic acid) and furfural. Moreover, lignin is most thermally stable among cellulose and hemicellulose. Pyrolysis of lignin produces higher char yield and lower liquid yield as compared to holocellulose,

liquid products obtained through the lignin pyrolysis mainly consist of larger molecular oligomers known as pyrolytic lignin, phenol-based compounds and lighter compounds such as methanol, HAA, acetic acid [57]. From the above discussion, it is accomplished that pyrolysis liquid is the mixture of various chemical compounds. Therefore, different chemical analysis such as FTIR, GC-MS and ^1H NMR is required to determine the chemical compositions of bio-oil.

Figure 7 shows the FTIR spectra of bio-oil. It provides information regarding the presence of several functional groups and chemical bonds in bio-oil. The broad strong peak observed at 3435 cm^{-1} is due to O-H stretching vibration and signifies the presence of alcohols and phenols [58]. The weak peak at 1718 cm^{-1} is due to C=O stretching vibration and corresponding to the presence of ketone and aldehyde groups [46]. The strong peak at 1634 cm^{-1} suggests the C=C stretching vibration due to the presence of alkenes and aromatics. The weak peak at around 1515 cm^{-1} representing C=C stretching vibration indicates the presence of alkenes and aromatics [59]. The peaks observed in between 1464 and 1378 cm^{-1} are due to C-H deformation and confirm the presence of alkanes [59]. Peaks in between 1275 and 1125 cm^{-1} indicate the C-O stretching, which specifies the existence of oxygenated compounds. In addition, peaks at 1100 and 1054 cm^{-1} represent the C-O stretching indicating the existence of ether [46]. The region between 900 and 700 cm^{-1} contains the weak peaks related to aromatic compounds with C-H bending [44]. The above FTIR result of present bio-oil is in agreement with other bio-oils described by the previous

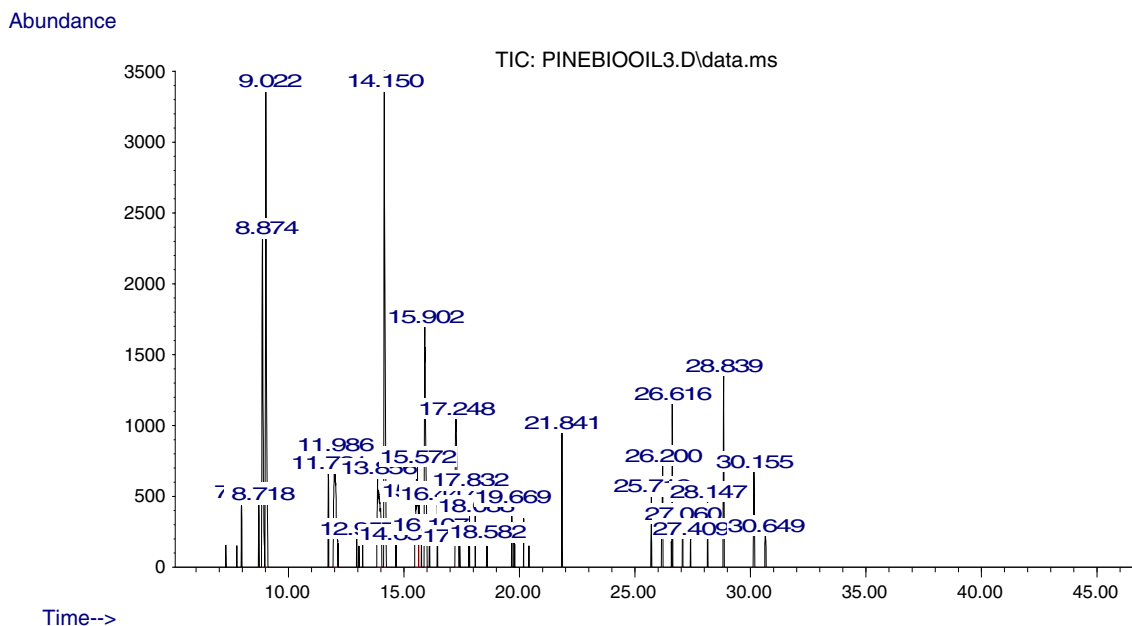


Fig. 8 GC-MS chromatogram of bio-oil

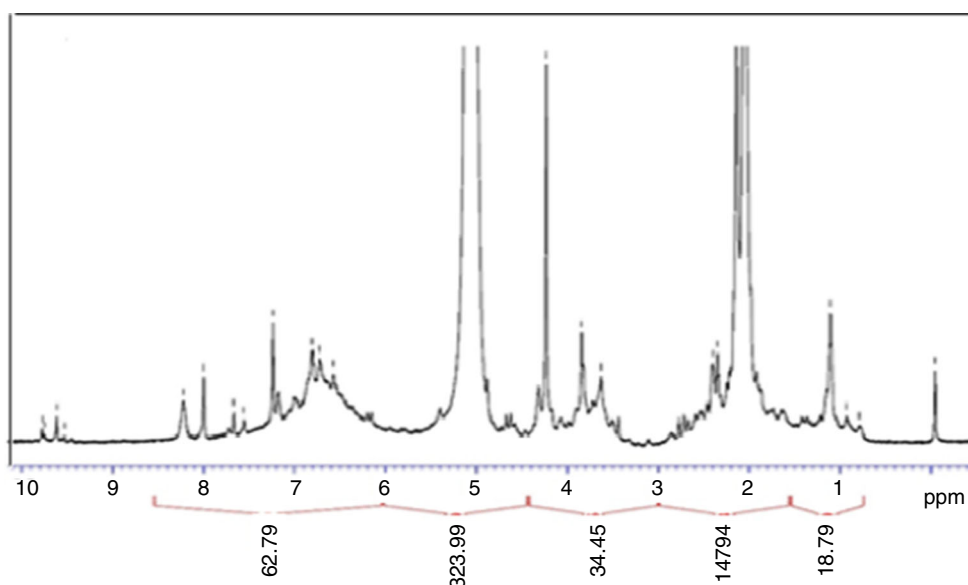
Table 4 Main chemical compounds present in bio-oil

Retention time/min	Peak area/%	Compound name	Molecular formula
8.72	1.01	1,6-Heptadiene	C ₇ H ₁₂
8.87	10.19	Propanamide, 2,2-dimethyl-	C ₅ H ₁₁ NO
9.02	12.45	2,3-Butanedione, monooxime	C ₄ H ₇ NO ₂
11.73	1.33	Phenol, 3-amino-	C ₆ H ₇ NO
11.99	7.09	Phenylephrine	C ₉ H ₁₃ NO ₂
13.86	5.25	1-Octen-3-yne	C ₈ H ₁₂
13.98	1.70	1,2-Cyclooctadiene	C ₈ H ₁₂
14.15	14.75	2-Acetyl-5-methylfuran	C ₇ H ₈ O ₂
15.57	5.92	Phenol, 4-ethyl-	C ₈ H ₁₀ O
15.65	2.48	Phenol, 2-ethyl-	C ₈ H ₁₀ O
15.90	8.75	2-Aminobenzyl alcohol	C ₇ H ₉ NO
17.25	7.42	Phenol, 4-ethyl-2-methoxy-	C ₉ H ₁₂ O ₂
21.84	2.01	Undecane, 5-methyl-	C ₁₂ H ₂₆
26.20	2.33	Benzamide, 2-methoxy-N-methyl-N-phenyl	C ₁₅ H ₁₅ NO ₂
26.62	2.76	Phenol, 4-(1H-pyrrol-1-yl)-	C ₁₀ H ₉ NO
28.84	3.41	Quinoline-4-carboxylic acid, 2-hydroxy-8-methoxy-	C ₁₁ H ₉ NO ₄
30.16	2.33	Benzenemethanamine, N-(1,3-benzodioxol-5-ylmethylidene)-	C ₁₅ H ₁₃ NO ₂

studies [46, 59]. The present FTIR analysis of bio-oil confirms the presence of various chemical compounds such as alkanes, alkenes, aromatics and several oxygen-containing compounds such as phenols, ketones, carboxylic acids or aldehydes. Further, to quantify the presence of different chemical compounds/groups in the bio-oil and also justify the existence of the above functional groups, bio-oil is also analyzed through GC–MS and ¹H NMR.

GC–MS is a very powerful technique used to detect the volatile chemical compounds presence in the bio-oil fraction with the help of difference in retention time in a column followed by difference in molecular mass of the compounds. The data signify that more than 50 compounds are present in the bio-oil and among these higher probable ($\geq 80\%$) compounds with major peaks are selected. Due to complex nature of bio-oil and limitation of MS library strength, it is not possible to clearly separate all the peaks. Figure 8 shows the GC–MS chromatogram of bio-oil, and Table 4 represents the list of chemical compounds present in the bio-oil, which have percentage peak area of greater than 1%, with their retention time, percentage peak area, compound name and molecular formula. On the basis of GC–MS results, aliphatic and aromatic hydrocarbons, phenols, furans, acids, alcohols, oxygenated compounds and nitrogenous compounds are prominent in the present bio-oil. The most significant compounds present in bio-oil are propanamide, 2,2-dimethyl; 2,3-butanedione, monooxime; phenylephrine; 1-octen-3-yne; 2-acetyl-5-methylfuran; phenol, 4-ethyl; 2-aminobenzyl alcohol; and phenol, 4-ethyl-2-methoxy with their relative composition of 10.19, 12.45, 7.09, 5.25, 14.75, 5.92, 8.75 and 7.42%, respectively. The carbon distribution range of the volatile chemical compounds present in bio-oil is C₄–C₁₅, which is comparable to the other petroleum fuels.

¹H NMR of bio-oil quantifies the presence of different types of protons based on the chemical shift with the selected regions as shown in Fig. 9. On the basis of chemical shifts for specific proton types, ¹H NMR spectrum can be categorized into three regions such as aliphatic, olefinic and aromatic. In particular, aliphatic, olefinic and aromatic resonances occur in the chemical shift region of 0.5–3.0, 4.5–6.3 and 6.0–9.0 ppm, respectively [60]. In

Fig. 9 ¹H NMR spectrum of bio-oil

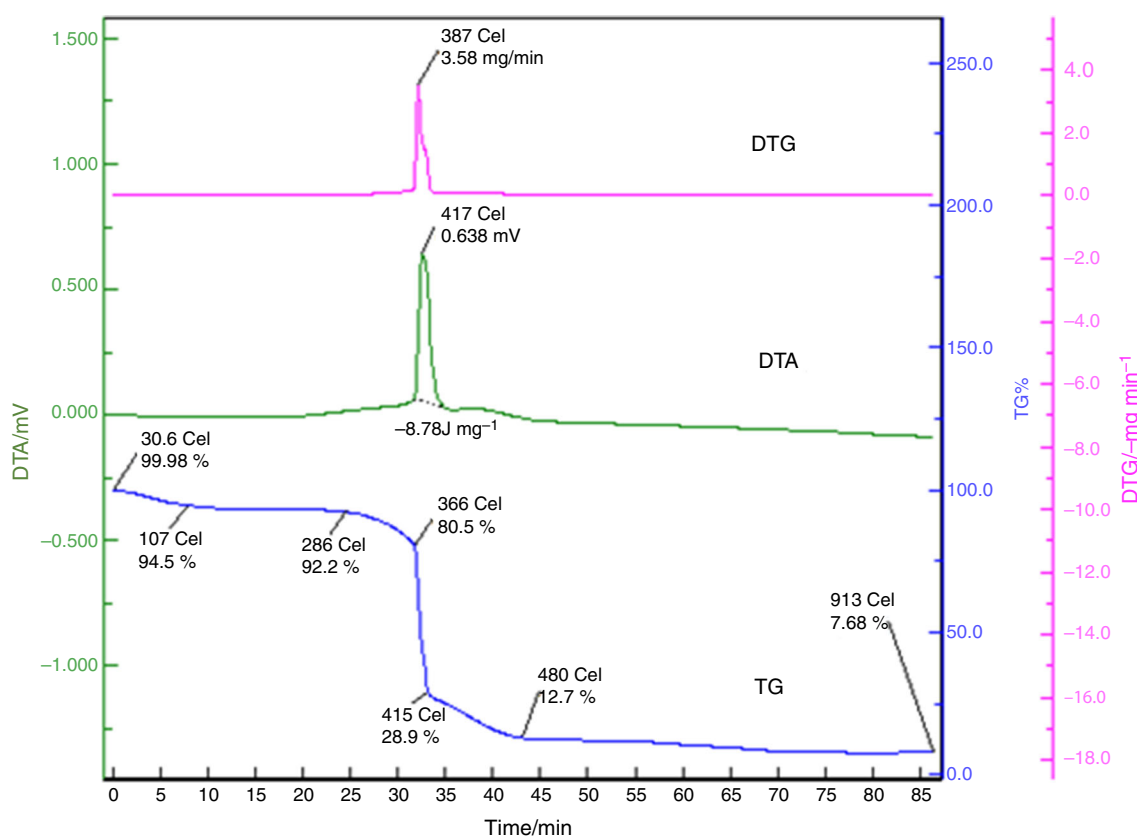


Fig. 10 TG/DTG/DTA curves of pine char at a heating rate of $10\text{ }^{\circ}\text{C min}^{-1}$

the present ^1H NMR spectrum of bio-oil, the region between 0.5 and 1.5 ppm around 3.2% of protons resonates due to the presence of aliphatic hydrocarbon chains [61]. In the next region from 1.5 to 3.0 ppm, it is observed that around 25.20% of protons resonate relates to protons on aliphatic carbon atoms, which may be bonded to unsaturated groups or heteroatoms [62]. The next region between 3.0 and 4.4 ppm is useful to identify the lignin derivatives, around 5.87% of protons resonate in this region. The region between 4.4 and 6 ppm is possibly due to the presence of protons, which are bonded to carbon atoms in methoxy or phenolic groups or carbohydrate-like molecules or olefins [54]. Around 55.03% protons resonate in this region for pine needles bio-oil. Finally, for aromatic region of the spectrum 6.0–8.5 ppm contains around 10.70% of protons. The above discussion quantifies the presence of alkanes, alkenes, aromatics and other chemical compounds such as phenols, alcohols and acids in the bio-oil, which is also in agreement with the FTIR analysis results.

Pyrolytic gas composition

Pyrolytic gas composition is determined by the chromatographic analysis. The relative composition of H_2 , CO_2 , CO and CH_4 in mol% at $550\text{ }^{\circ}\text{C}$ is found as 10.16, 45.62, 30.12

and 14.10%, respectively. Carbon monoxide and hydrogen can be utilized as syngas for liquid fuel production as well as hydrogen can also be used for upgradation of bio-oil.

Characteristics of bio-char

Bio-char produced by the pyrolysis of biomass can be utilized as the solid fuel, cheap adsorbent, carbon sequestration and soil amendment. It can also be used for production of household briquette and activated carbon. So, various characterizations of bio-char have been done to find out its potential for applications through suitable route as mentioned above. Table 1 shows the proximate, ultimate analysis and heating value of bio-char.

Moisture content of present bio-char is 1.14%. This is because of the absorption of some moisture, when it is exposed to air. Volatile matter of pine needles is 77.55%, which significantly reduces to 18.36% after pyrolysis. It is due to the conversion of volatile matter into liquid and gaseous products. As a result of decrease in volatile matter, the fixed carbon content increases to 65.34%. The ash content in bio-char is 15.16%. Ultimate analysis result shows that bio-char becomes carbonaceous with carbon content of 69.83%. From Table 1, it is observed that there are significant variations in carbon and oxygen content and

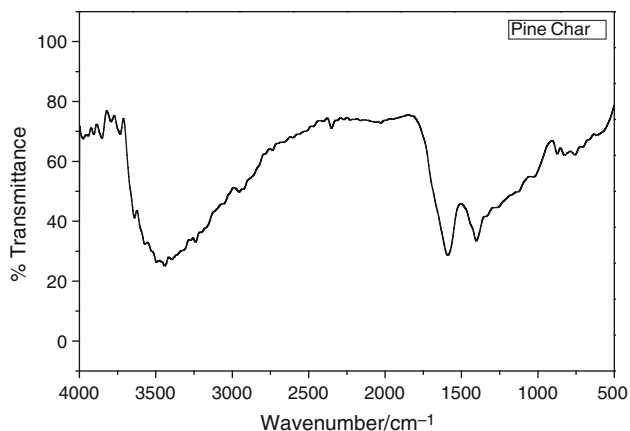
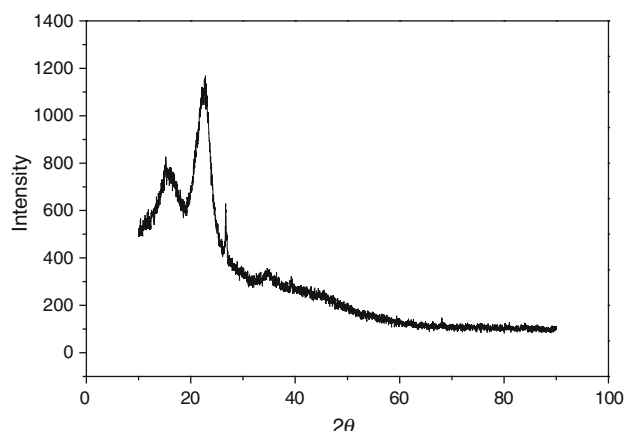


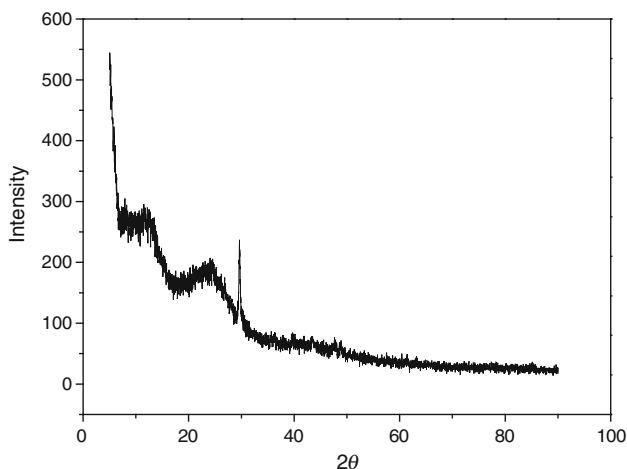
Fig. 11 FTIR spectra of bio-char

slight variations in hydrogen, nitrogen and sulfur content between pine needles and their bio-char. The bio-char has higher carbon content and lower oxygen content as compared to pine needles. This signifies the removal of oxygen and other volatile compounds, which increases the carbon content [47]. The N and S contents in bio-char are low as 1.07 and 0.03%, respectively. The H/C and O/C molar ratio of bio-char is lower than original biomass; it signifies the loss of H and O due to various reactions such as dehydration, decarbonylation and decarboxylation during pyrolysis [48]. Due to these reactions, oxygen-containing functional groups are decomposed and transformed into the alkyl-aryl C–C bonds as a cross-linking between small aromatic rings [29]. Thus, increase in calorific value of bio-char (25.50 MJ Kg^{-1}) is achieved as compared to original biomass (19.65 MJ Kg^{-1}). The empirical formula of bio-char is $\text{CH}_{0.56}\text{O}_{0.28}\text{N}_{0.013}$. The above analysis of bio-char suggests that it has potential to be used as solid fuel. The pH of bio-char is found to be 9.8; it is alkaline in nature, because during pyrolysis removal of organic matter takes place, which increases the concentration of alkali [63]. The pH is an important property of soil, which affects the types of plants and microbes to thrive and the availability of nutrients to be absorbed. Acidity in the soil increases due to the result of nitric and sulfuric acid from fossil fuel combustion and continuous use of nitrogenous fertilizers [64, 65]. Thus, due to the alkaline nature of bio-char, it can be used for soil amendment to neutralize the soil acidity and increase soil pH as well as to improve the soil quality and raise the crop productivity [54].

Figure 10 shows the TG, DTG and DTA curves of bio-char in oxidizing atmosphere. It is shown from TG curve that thermal degradation behavior of bio-char can be divided into four stages. From temperature 30 to 150 °C, mass loss related to the removal of moisture and some extractives from bio-char. Mass loss of around $\sim 10\%$ occurs in the temperature range of 150–315 °C is due to the



(a)



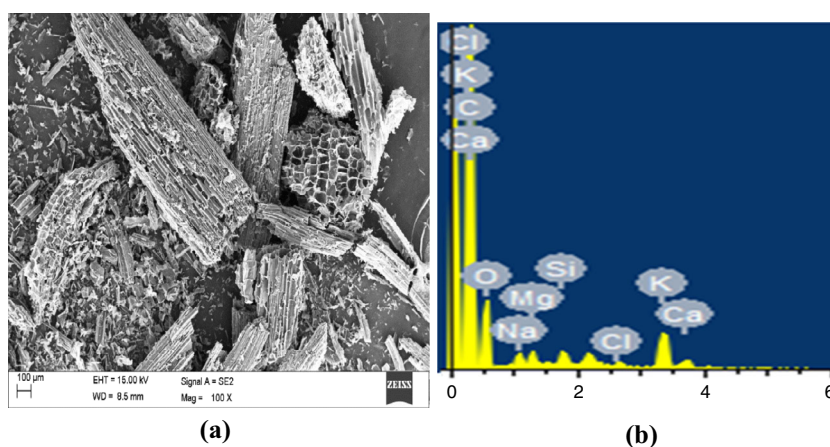
(b)

Fig. 12 X-ray diffractogram of **a** pine needles, **b** bio-char

oxidation of remaining hemicellulose [66]. The main mass loss of around 70% occurs within the temperature range of 350–480 °C, which is due to the oxidation of cellulose and some lignin. DTG curve signifies the maximum mass loss rate of 3.58 mg min^{-1} at the temperature of 387 °C, and DTA curve shows the exothermic peak at temperature of around 417 °C with heat release of 8.78 J mg^{-1} . Above 480 °C mass loss is very low, which is due to the oxidation of remaining lignin. Thermal analysis of bio-char suggests that the combustion of bio-char releases significant amount of heat, so it can be used as fuel, alone or mixed with other fuel for energy generation through combustion [66].

Figure 11 shows the FTIR spectra of bio-char, which demonstrates the peaks between 3000 and 3600 cm^{-1} assigned to the vibration of O–H group; it signifies the presence of hydroxyl groups [67]. Peak at around 1600 cm^{-1} might be due to the C=C stretching, and this provides the existence of alkenes and aromatics in present bio-char [8, 68]. Peak at 1510 cm^{-1} is due to the aromatic ring vibration which implies the presence of lignin [61].

Fig. 13 **a** FESEM image of bio-char at 100× magnification, **b** EDX spectra of bio-char



Weak peak at 1396 cm^{-1} attributes to the C–H bending vibration due to the presence of alkanes [61]. The peaks present in spectra between 1000 and 800 cm^{-1} are due to aromatic rings and C–H alkynes bonds [69]. Hence, it is found that bio-char significantly loses aliphatic and hydroxyl groups and gains the aromatic character.

X-ray diffractogram of raw pine needles and bio-char is shown in Fig. 12a, b, respectively. XRD analysis is relevant technique to analyze the crystallinity of a material [70]. The XRD spectra of pine needles show two sharp peaks at 2θ of around 16° and 22° and signify the crystalline region of cellulose present in the biomass [71]. However, hemicellulose and lignin are also present in biomass, but they are amorphous in nature. After the pyrolysis of pine needles, it partially loses the crystalline structure of cellulose and the intensity of two peaks decreases and becomes broader as well as 2θ value also shifted slightly (23°) for bio-char as shown in Fig. 12b, which indicates the degradation of cellulose during pyrolysis.

Surface morphology of bio-char is described by FESEM image as shown in Fig. 13a at 100× magnification. FESEM images confirm the rough texture and heterogeneous structure of bio-char. It is also observed that the rough surface of bio-char has many heterogeneous pores, which indicates that it may be used as adsorbent. The removal of volatile matters from biomass during pyrolysis creates pores at the surface of bio-char [72]. Highly porous bio-chars have more numbers of adsorption sites for ions and offer spaces for water and nutrients/pollutants retention. Figure 13b represents the EDX analysis of bio-char. It is observed from the EDX analysis that bio-char consists of various inorganic matters such as Na, Mg, Si, K and Ca and these are the important nutrients for soil fertility and to improve the crop productivity [33]. Hence, it can be also used as fertilizer. For the present bio-char, BET surface area, pore volume and average pore size are found to be $10.85\text{ m}^2\text{ g}^{-1}$, $0.011\text{ cm}^3\text{ g}^{-1}$ and 4.37 nm , respectively.

Low value of BET surface area of bio-char is due to the shrinkage of chars at post-softening and swelling temperatures, resulting in narrowing or closing the pores. The surface area and quality of bio-char can be improved by acid and alkaline activation for its use in adsorption process. Further, it can also be converted to activated carbon after physical and chemical activation process.

Conclusions

In this study, pyrolysis experiments of pine needles were conducted in a semi-batch reactor to study the effect of pyrolysis temperature, heating rate, N_2 flow rate and particle size on the products yield. The maximum bio-oil yield of 43.76% is found at temperature of $550\text{ }^\circ\text{C}$, heating rate of $50\text{ }^\circ\text{C min}^{-1}$ and at N_2 flow rate of $100\text{ cm}^3\text{ min}^{-1}$ for biomass particle size of $0.6 < d_p < 1\text{ mm}$. Bio-oil has an empirical formula of $\text{CH}_{1.47}\text{O}_{0.36}\text{N}_{0.005}$, carbon distribution range of $\text{C}_4\text{--C}_{15}$ and HHV of 26.25 MJ kg^{-1} . The results of spectroscopic and chromatographic analysis suggest the presence of aliphatic, olefinic and aromatic as well as many oxygenated compounds in bio-oil. This bio-oil can be used for fuel application after refining and upgrading. It can also be used as a feedstock for valuable chemicals production. Bio-char has high carbon content with HHV of 25.50 MJ kg^{-1} , so it can be useful for energy application and as a precursor for activated carbon production. FESEM, EDX and BET surface area analysis showed that bio-char surface has porous structure and contains various nutrients. It can be used as an adsorbent in water purification process and provide nutrient for soil. Due to the high pH of bio-char, it can also be used for soil amendment to neutralize soil acidity and increase the soil pH. The gaseous products have carbon monoxide and hydrogen, which can be further used as fuel or to synthesize into liquid fuels. Moreover, hydrogen can be used for upgrading of the bio-oil. The present study concludes that pine needles are a

good source of renewable energy, which can be sustained if all the pyrolysis products are utilized efficiently.

References

1. Antal MJJ, Varhegyi G. Cellulose pyrolysis kinetics: the current state of knowledge. *Ind Eng Chem Res.* 1995;34:703–17.
2. Zhang L, Xu CC, Champagne P. Overview of recent advances in thermo-chemical conversion of biomass. *Energy Convers Manag.* 2010;51:969–82.
3. Morali U, Şensöz S. Pyrolysis of hornbeam shell (*Carpinus betulus* L.) in a fixed bed reactor: characterization of bio-oil and bio-char. *Fuel.* 2015;150:672–8.
4. Demiral İ, Şensöz S. Fixed-bed pyrolysis of hazelnut (*Corylus avellana* L.) bagasse: influence of pyrolysis parameters on product yields. *Energy Source Part A.* 2006;28:1149–58.
5. Raveendran K, Ganesh A, Khilar KC. Pyrolysis characteristics of biomass and biomass components. *Fuel.* 1996;75:987–98.
6. Varma AK, Mondal P. Physicochemical characterization and kinetic study of pine needle for pyrolysis process. *J Therm Anal Calorim.* 2015;124:487–97.
7. Shafizadeh F. Introduction to pyrolysis of biomass. *J Anal Appl Pyrolysis.* 1982;3:283–305.
8. Saikia R, Chutia RS, Katak R, Pant KK. Perennial grass (*Arundo donax* L.) as a feedstock for thermo-chemical conversion to energy and materials. *Bioresour Technol.* 2015;188:265–72.
9. Akhtar J, Amin NS. A review on operating parameters for optimum liquid oil yield in biomass pyrolysis. *Renew Sustain Energy Rev.* 2012;16:5101–9.
10. Ningbo G, Baoling L, Aimin L, Juanjuan L. Continuous pyrolysis of pine sawdust at different pyrolysis temperatures and solid residence times. *J Anal Appl Pyrolysis.* 2015;114:155–62.
11. Salehi E, Abedi JT. Harding, bio-oil from sawdust: pyrolysis of sawdust in a fixed-bed system. *Energy Fuels.* 2009;23:3767–72.
12. Becidan M, Várhegyi G, Hustad JE, Skreiberg O. Thermal decomposition of biomass wastes. A kinetic study. *Ind Eng Chem Res.* 2007;46:2428–37.
13. Yorgun S, Şensöz S, Koçkar ÖM. Characterization of the pyrolysis oil produced in the slow pyrolysis of sunflower-extracted bagasse. *Biomass Bioenergy.* 2001;20:141–8.
14. Hernandez-Mena LE, Pécora AA, Beraldob AL. Slow pyrolysis of bamboo biomass: analysis of biochar properties. *Chem Eng.* 2014;37:115–20.
15. Chouhan APS. A slow pyrolysis of cotton stalk (*Gossypium arboretum*) waste for bio-oil production. *J Pharm Chem Biol Sci.* 2015;3:143–9.
16. Mohammed IY, Abakr YA, Kazi FK, Yusuf S, Alshareef I, Chin SA. Pyrolysis of napier grass in a fixed bed reactor: effect of operating conditions on product yields and characteristics. *BioResources.* 2015;10:6457–78.
17. Suttibak S, Sriprateep K, Pattiya A. Production of bio-oil from pine sawdust by rapid pyrolysis in a fluidized-bed reactor. *Energy Source Part A.* 2015;37:1440–6.
18. Lazzari E, Schena T, Primaz CT, da Silva Maciel GP, Machado ME, Cardoso CAL, Jacques RA, Caramão EB. Production and chromatographic characterization of bio-oil from the pyrolysis of mango seed waste. *Ind Crops Prod.* 2016;83:529–36.
19. Wagenaar BM, Prins W, Swaaij VW. Flash pyrolysis kinetics of pine wood. *Fuel Process Technol.* 1993;3:6291–8.
20. Chen D, Zhou J, Zhang Q. Effects of heating rate on slow pyrolysis behavior, kinetic parameters and products properties of moso bamboo. *Bioresour Technol.* 2014;169:313–9.
21. Liu Z, Zhang FS, Wu J. Characterization and application of chars produced from pinewood pyrolysis and hydrothermal treatment. *Fuel.* 2010;89:510–4.
22. Özbay G. Catalytic pyrolysis of pine wood sawdust to produce bio-oil: effect of temperature and catalyst additives. *J Wood Chem Technol.* 2015;35:302–13.
23. Westerhof RJ, Brilman DWF, Garcia-Perez M, Wang Z, Oudenhoven SR, Kersten SR. Stepwise fast pyrolysis of pine wood. *Energy Fuels.* 2012;26:7263–73.
24. Dhaundiyal A, Gangwar J. Kinetics of the thermal decomposition of pine needles. *Acta Univ Sapientiae Agric Environ.* 2015;7:5–22.
25. Font R, Conesa JA, Moltó J, Muñoz M. Kinetics of pyrolysis and combustion of pine needles and cones. *J Anal Appl Pyrolysis.* 2009;85:276–86.
26. Safi MJ, Mishra IM, Prasad B. Global degradation kinetics of pine needles in air. *Thermochim Acta.* 2004;412:155–62.
27. Statheropoulos M, Lioudakis S, Tzamtzis N, Pappa A, Kyriakou S. Thermal degradation of *pinus halepensis* pine-needles using various analytical methods. *J Anal Appl Pyrolysis.* 1997;43:115–23.
28. Varma AK, Mondal P. Physicochemical characterization and pyrolysis kinetic study of sugarcane bagasse using thermogravimetric analysis. *J Energy Resour Technol.* 2016;138:052205.
29. Kim P, Johnson A, Edmunds CW, Radosevich M, Vogt F, Rials TG, Labbe N. Surface functionality and carbon structures in lignocellulosic-derived biochars produced by fast pyrolysis. *Energy Fuels.* 2011;25:4693–703.
30. Asadullah M, Rahman MA, Ali MM, Rahman MS, Motin MA, Sultan MB, Alam MR. Production of bio-oil from fixed-bed pyrolysis of bagasse. *Fuel.* 2007;86:2514–20.
31. Jeguirim M, Trouvé G. Pyrolysis characteristics and kinetics of *Arundo donax* using thermogravimetric analysis. *Bioresour Technol.* 2009;100:4026–31.
32. Ackalın K. Pyrolytic characteristics and kinetics of pistachio shell by thermogravimetric analysis. *J Therm Anal Calorim.* 2012;109:227–35.
33. Chutia RS, Katak R, Bhaskar T. Characterization of liquid and solid product from pyrolysis of *Pongamia glabra* deoiled cake. *Bioresour Technol.* 2014;165:336–42.
34. Şensöz S, Demiral İ, Gerçel HF. Olive bagasse (*Olea europea* L.) pyrolysis. *Bioresour Technol.* 2006;97:429–36.
35. Encinar JM, Gonzalez JF, Gonzalez J. Fixed-bed pyrolysis of *Cynara cardunculus* L. Product yields and compositions. *Fuel Process Technol.* 2000;68:209–22.
36. Haykiri-Acma H. The role of particle size in the non-isothermal pyrolysis of hazelnut shell. *J Anal Appl Pyrolysis.* 2006;75:211–6.
37. Uzun BB, Pütün AE, Pütün E. Fast pyrolysis of soybean cake: product yields and compositions. *Bioresour Technol.* 2006;97:569–76.
38. Maggi R, Delmon B. Comparison between slow and flash pyrolysis oils from biomass. *Fuel.* 1994;73:671–7.
39. Acıkgöz C, Onay O, Kockar OM. Fast pyrolysis of linseed: product yields and compositions. *J Anal Appl Pyrolysis.* 2004;71:417–29.
40. Ekinçi E, Citiroglu M, Putun E, Love GD, Lafferty CJ, Snapet CE. Effect of lignite addition and steam on the pyrolysis of Turkish oil shales. *Fuel.* 1992;71:1511–4.
41. Majhi A, Sharma YK, Naik DV, Chauhan R. The production and evaluation of bio-oil obtained from the *Jatropha curcas* cake. *Energy Source Part A.* 2015;37:1782–9.
42. Yorgun S, Yıldız D. Slow pyrolysis of paulownia wood: effects of pyrolysis parameters on product yields and bio-oil characterization. *J Anal Appl Pyrolysis.* 2015;114:68–78.

43. Şensöz S, Angın D. Pyrolysis of safflower (*Charthamustinctorius* L.) seed press cake: part 1. The effects of pyrolysis parameters on the product yields. *Bioresour Technol.* 2008;99:5492–7.
44. Rout T, Pradhan D, Singh RK, Kumari N. Exhaustive study of products obtained from coconut shell pyrolysis. *J Environ Chem Eng.* 2016;4:3696–705.
45. Demiral I, Ayan EA. Pyrolysis of grape bagasse: effect of pyrolysis conditions on the product yields and characterization of the liquid product. *Bioresour Technol.* 2011;102:3946–51.
46. Lee MK, Tsai WT, Tsai YL, Lin SH. Pyrolysis of napier grass in an induction-heating reactor. *J Anal Appl Pyrolysis.* 2010;88:110–6.
47. Singh VK, Soni AB, Kumar S, Singh RK. Pyrolysis of sal seed to liquid product. *Bioresour Technol.* 2014;151:432–5.
48. Yakub MI, Abdalla AY, Feroz KK, Suzana Y, Ibraheem A, Chin SA. Pyrolysis of oil palm residues in a fixed bed tubular reactor. *J Power Energy Eng.* 2015;31:85–93.
49. Pradhan D, Singh RK, Bendu H, Mund R. Pyrolysis of mahua seed (*Madhucaindica*)—production of bio-fuel and its characterization. *Energy Convers Manag.* 2016;108:529–38.
50. Mantilla SV, Gauthier-Maradei P, Gil PÁ, Cárdenas ST. Comparative study of bio-oil production from sugarcane bagasse and palm empty fruit bunch: yield optimization and bio-oil characterization. *J Anal Appl Pyrolysis.* 2014;108:284–94.
51. Azargohar R, Jacobson KL, Powell EE, Dalai AK. Evaluation of properties of fast pyrolysis products obtained from Canadian waste biomass. *J Anal Appl Pyrolysis.* 2013;104:330–40.
52. Lu Q, Yang X, Zhu X. Analysis on chemical and physical properties of bio-oil pyrolyzed from rice husk. *J Anal Appl Pyrolysis.* 2008;82:191–8.
53. Abnisa F, Arami-Niya A, Daud WW, Sahu JN, Noor IM. Utilization of oil palm tree residues to produce bio-oil and bio-char via pyrolysis. *Energy Convers Manag.* 2013;76:1073–82.
54. Bordoloi N, Narzari R, Chutia RS, Bhaskar T, Katak R. Pyrolysis of *Mesua ferrea* and *Pongamia glabra* seed cover: characterization of bio-oil and its sub-fractions. *Bioresour Technol.* 2015;178:83–9.
55. Islam MR, Haniu H, Islam MN, Uddin MS. Thermochemical conversion of sugarcane bagasse into bio-crude oils by fluidized-bed pyrolysis technology. *J Therm Sci Technol.* 2010;5:11–23.
56. Islam MR, Islam MN, Nabi MN. Bio-crude oil from fluidized bed pyrolysis of rice-straw and its characterization. *Int Energy J.* 2002;3:1–11.
57. Chen D, Chen X, Sun J, Zheng Z, Fu K. Pyrolysis polygeneration of pine nut shell: quality of pyrolysis products and study on the preparation of activated carbon from biochar. *Bioresour Technol.* 2016;216:629–36.
58. Chen W, Shi S, Zhang J, Chen M, Zhou X. Co-pyrolysis of waste newspaper with high-density polyethylene: synergistic effect and oil characterization. *Energy Convers Manag.* 2016;112:41–8.
59. Tsai WT, Lee MK, Chang YM. Fast pyrolysis of rice straw, sugarcane bagasse and coconut shell in an induction-heating reactor. *J Anal Appl Pyrolysis.* 2006;76:230–7.
60. Stütçü H, Toroglu I, Piskin S. Structural characterization of oil component of high temperature pyrolysis tars. *Energy Sources.* 2005;27:521–34.
61. Balagurumurthy B, Srivastava V, Kumar J, Biswas B, Singh R, Gupta P, Kumar KS, Singh R, Bhaskar T. Value addition to rice straw through pyrolysis in hydrogen and nitrogen environments. *Bioresour Technol.* 2015;188:273–9.
62. Mullen CA, Strahan GD, Boateng AA. Characterization of various fast-pyrolysis bio-oils by NMR spectroscopy. *Energy Fuels.* 2009;23:2707–18.
63. Lee Y, Park J, Ryu C, Gang KS, Yang W, Park YK, Jung J, Hyun S. Comparison of biochar properties from biomass residues produced by slow pyrolysis at 500 °C. *Bioresour Technol.* 2013;148:196–201.
64. Reuss JO, Johnson DW. Effect of soil processes on the acidification of water by acid deposition. *J Environ Qual.* 1985;14:26–31.
65. Malhi SS, Nyborg M, Harapiak JT. Effects of long-term N fertilizer-induced acidification and liming on micronutrients in soil and in brome grass hay. *Soil Tillage Res.* 1998;48:91–101.
66. Sellin N, Krohl DR, Marangoni C, Souza O. Oxidative fast pyrolysis of banana leaves in fluidized bed reactor. *Renew Energy.* 2016;96:56–64.
67. Yang H, Yan R, Chen H, Lee DH, Zheng C. Characteristics of hemicellulose, cellulose and lignin pyrolysis. *Fuel.* 2007;86:1781–8.
68. Boon JJ, Pastorova I, Botto RE, Arisz PW. Structural studies on cellulose pyrolysis and cellulose chars by PYMS, PYGCMS, FTIR, NMR and by wet chemical techniques. *Biomass Bioenergy.* 1994;7:25–32.
69. Tinwala F, Mohanty P, Parmar S, Patel A, Pant KK. Intermediate pyrolysis of agro-industrial biomasses in bench-scale pyrolyser: product yields and its characterization. *Bioresour Technol.* 2015;188:258–64.
70. Ertas M, Alma MH. Pyrolysis of laurel (*Laurusnobilis* L.) extraction residues in a fixed-bed reactor: characterization of bio-oil and bio-char. *J Anal Appl Pyrolysis.* 2010;88:22–9.
71. Yang Z, Jiang ZH, So CL, Hse CY. Rapid prediction of wood crystallinity in *Pinus elliotii* plantation wood by near-infrared spectroscopy. *J Wood Sci.* 2007;53:449–53.
72. Yao Y, Gao B, Inyang M, Zimmerman AR, Cao X, Pullamanappallil P, et al. Biochar derived from anaerobically digested sugar beet tailings: characterization and phosphate removal potential. *Bioresour Technol.* 2011;102:6273–8.